Available online at www.sciencedirect.com

ScienceDirect

Physics Procedia 83 (2016) 114 – 122

Physics Procedia

9th International Conference on Photonic Technologies - LANE 2016

Influence of the liquid on femtosecond laser ablation of iron

A. Kanitz[a], J.S. Hoppius[a], E.L. Gurevich[a], A. Ostendorf[a,*]

[a]*Ruhr-Universität Bochum, Universitätsstr. 150, 44801 Bochum, Germany*

Abstract

Ultrashort pulse laser ablation has become a very important industrial method for highly precise material removal ranging from sensitive thin film processing to drilling and cutting of metals. Over the last decade, a new method to produce pure nanoparticles emerged from this technique: Pulsed Laser Ablation in Liquids (PLAL). By this method, the ablation of material by a laser beam is used to generate a metal vapor within the liquid in order to obtain nanoparticles from its recondensation process. It is well known that the liquid significantly alters the ablation properties of the substrate, in our case iron. For example, the ablation rate and crater morphology differ depending on the used liquid. We present our studies on the efficiency and quality of ablated grooves in water, methanol, acetone, ethanol and toluene. The produced grooves are investigated by means of white-light interferometry, EDX and SEM.

Peer-review under responsibility of the Bayerisches Laserzentrum GmbH

Keywords: laser ablation; liquids; femtosecond

1. Introduction

Over the last years, ultrashort pulse laser ablation has become an more important industrial tool in different fields like thin film processing, microstructuring and nanoparticle production (Barcikowski et al. (2013)).

Three parameters yield information on the ablation process. First, the ablation rate is a direct measure for the efficiency of the material removal process. Second, the macro- and microstructure give indications on the melting and spallation process through the resolidification of the molten material vapor (Shen et al. (2004)). In addition, the microstructure is important for the quality of the ablation process. Third, through the interaction of the molten

* Corresponding author. Tel.:+49-234-3223932 .
E-mail address: kanitz@lat.rub.de

Peer-review under responsibility of the Bayerisches Laserzentrum GmbH
doi:10.1016/j.phpro.2016.08.022

material of the ablation process with the surrounding environment, the surface can be chemically modified. Thus, this surface modification yields information on the chemistry and it needs to be considered for any ablation process, since it can alter the substrate's composition und thus its properties (Schaaf (2002)). Depending on the application, ultrashort pulsed laser ablation in liquids (PLAL) can provide benefits for all of those factors (Muhammad et al. (2012), Zhang et al. (2016) and Kruusing (2004)) and additionally generate highly surface clean nanoparticles directly in a liquid suspension with enhanced surface chemistry (Wagener et al. (2012)).

Due to the complex physico-chemical interactions, PLAL remains a topic of investigation. In this proceeding, we investigate the ablation of grooves of pure iron in different liquids to evaluate the influence of the laser parameters on the ablation rate, macro- and microstructure (groove morphology) as well as chemical surface modification.

Here, iron is a material of interest because it is reactive, magnetic and an important component of many alloys. This investigation may serve to understand the controllability of iron-based nanoparticle generation in liquids by laser parameters as well as surface processing of iron-based materials in different liquids.

Accordingly to Nolte et al. (1997) and Neuenschwander et al. (2012), the ablation rate and quality of the ablation process is dependent on the applied fluence. Two fluences regimes exist which are determined by a different characteristic ablation depth. On the one hand, the ablation depth of the first regime at low fluences is determined by the optical penetration depth. Usually, the applied fluences for this regime are below 1 J/cm². On the other hand, the ablation depth in the second regime is determined by the thermal penetration depth caused by electron heat conduction. In addition, the second ablation regime leads to an increase of internal pressure within the material and higher ablation rates (Zhigilei et al. (2012), Nedialkov et al. (2004)). The threshold for this regime is usually above 1 J/cm². In order to investigate the influence of the different fluence regimes, it was chosen to work at two specific fluences; a low fluence of 0.2 J/cm², which yields the optimal ablation rate for our experimental system (Kanitz et al. (2015)) and a high fluence of 5 J/cm² which is well above the threshold value for the second ablation regime.

In order to evaluate the change of the local environment by the influence of previous pulses during ablation, the influence of different overlapping rates (OR) at a fixed repetition rate (5 KHz) is studied. The OR were chosen to be 0 %, 50 % and 90 % and controlled by changing the scanning rate. Usually, overlapping for PLAL should be avoided due to cavitation bubbles which may reflect the incoming laser beam and reduce the ablation rate (Wagner et al. (2010)). However, the used laser system possesses a repetition rate of 5 KHz with a temporal interpulse distance of 200 µs. Within this interpulse delay, the cavitation bubble should be mostly disappeared (de Bonis et al. (2015), Wagner et al. (2010)). Since, the cavitation bubble dynamics were not measured, a possible influence of the cavitation bubble cannot be ruled out completely. De Bonis et al. stated that a cavitation bubble for iron in water does only last about 100 µs whereas in acetone rebound events occur that may prolong the time window of interaction of the laser beam with the cavitation bubble up to 200 µs. Despite the interaction of the laser beam with the cavitation bubble, the laser beam also interacts with the ablated material which is still confined in the ablation area. This effect is usually referred to as particle shielding. For the experiments, five different liquids of highly pure water, methanol, ethanol, acetone and toluene which are commonly used for nanoparticle production were used.

2. Experimental procedure

The grooves were created by laser pulses of a Spectra-Physics Spitfire Ace System as laser source. A 5 W system with minimal pulse duration of 35 fs and repetition rate of 5 kHz resulting in maximal pulse energy of 1 mJ per pulse at a central wavelength of 800 nm. The power of the laser beam is controlled by a λ/2-waveplate in combination with a polarizing beam splitter. Further, the beam was guided through a galvo-scanner and an 80 mm telecentric lens onto the iron target which was covered by a liquid with a height of 4 mm. The targets consisted of 99.5 % pure Fe sheets with a thickness of 0.5 mm. The target and scanner were connected to an x-y-z nanopositioning system that allows precise control of the laser beam position on the target.

The pulse energy was kept constant at 800 µJ while the applied fluence on the target was changed by defocusing allowing a careful adjustment of the fluence. In order to avoid any influence and possible energy loss by an optical breakdown within the liquid, the target was always moved towards the focusing lens with the focus always being in the target.

A groove with a length of 5 mm was cut into the substrate with a total number of 10k shots so that the same amount of energy was deposited onto the substrate. To reach the number of 10k shots, the grooves were processed

by multi-passing with a delay of 1 s between each pass to avoid particle shielding from prior passes. An estimation of the diffusion time for molecular species indicates that within this time most of the ablation products of the prior shot should be diffused out of the ablation zone.

The ablated volume was measured by a white-light interferometer (TMS-1200 Polytec) with up to 10 nm sample increment resolution. For the determination of surface modifications, EDX mapping measurements were employed. Due the unknown penetration depth of the electron beam into the material, these mappings only consist in qualitative measurements.

3. Results

3.1. Ablation rate in different liquids

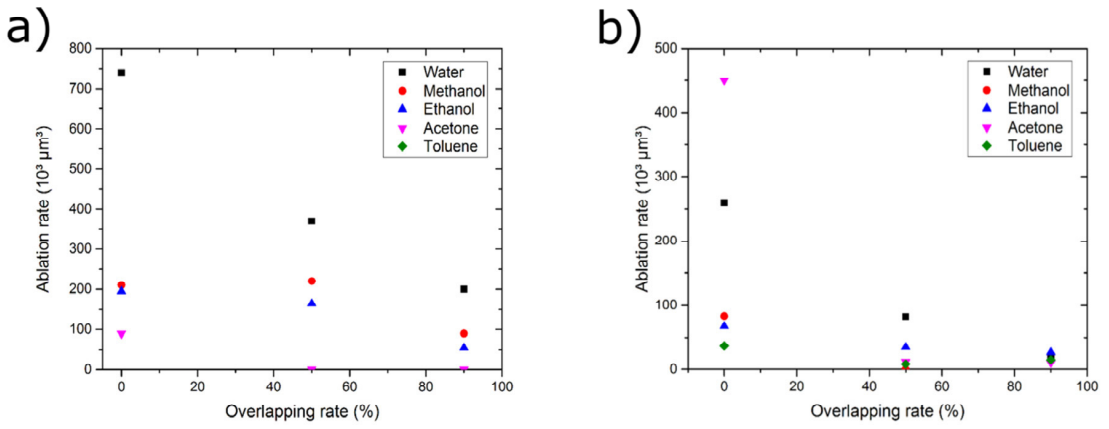

Fig. 1. Ablated volume of the groove at different overlapping rates a) at 0.2 J/cm², b) at 5 J/cm².

Fig. 1 shows the ablation rate for the investigated fluences of a) 0.2 J/cm² and b) 5 J/cm² for the different OR and liquids. Note that the ablation rate of toluene was not measurable at 0.2 J/cm². Except for acetone at 5 J/cm² and 0 % OR, the best ablation efficiency is always obtained in water. The unusually high ablation rate of acetone at 5 J/cm² cannot be explained easily but a possible explanation will be given in the following chapter based on the findings of the microstructure of the groove.

While the ablation rate is steadily decreasing with increasing overlap in water, organic liquids exceed a far more complex behavior. For example at 0.2 J/cm², the ablation rate of methanol and ethanol is barely affected at 50 % OR and a bit at 90 % OR while in acetone the ablation decreases strongly already for 50 % OR.

For the case of methanol, this behavior is different at 5 J/cm² where the ablation rate, similar to acetone strongly decreases with increasing OR. In contrast, the ablation rate in ethanol is much less affected. Furthermore, it should be noted that the ablation rate in toluene is bigger at 5 J/cm² than at 0.2 J/cm² which is contrary to all other investigated liquids where the ablation rate at 5 J/cm² is smaller than at 0.2 J/cm².

On the one hand, the different ablation rates between the liquids cannot be explained by conventional liquid properties like viscosity, density or surface tension etc.. On the other hand, the different ablation rate behavior with increasing OR might be explained by two factors; particle shielding (slow decrease) and cavitation bubble decrease (strong shielding due to beam deflection). However, a proof by ultrafast spectroscopic techniques is required for confirmation.

To sum up, the ablation rates are strongly affected by fluence and OR. Especially, the ablation behavior at different OR is fluence dependent. Due to the different dependency of the ablation rate on the OR, it is likely that the ablation rate is changed by multiple mechanisms, probably, an interaction with the cavitation bubble, particle

shielding and a hot liquid environment. To find out more about the ablation process, a more detailed investigation on the surface chemistry and ablation morphology is provided within the next chapters.

3.2. Properties of ablation in Water

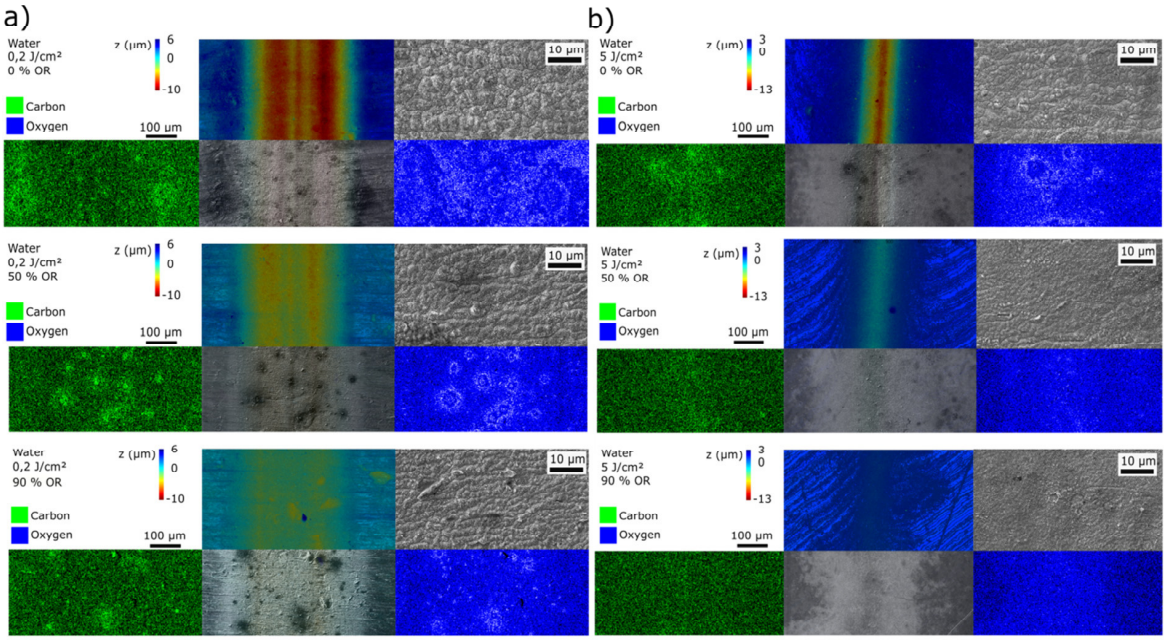

Fig. 2. Properties of the ablated grooves in water at a) 0.2 J/cm², b) 5 J/cm².

Fig. 2 shows the different properties of the ablated grooves in water which are indicated by a white-light interferometer picture in the upper middle with the corresponding SEM picture below and the chemical EDX analysis for oxygen and carbon at the right and left side, respectively. The upper right corner of one series provides an SEM picture with higher resolution to observe the laser induced microstructure which preferably originates from the resolidifaction of expelled molten layers and accumulation effects that are typical features of PLAL (de Bonis et al. (2013), Mannion et al. (2004)). For a better comparison, this presentation template is the same for all investigated liquids.

For a fluence of 0.2 J/cm², the ablated grooves do not exhibit a homogenously ablated area as expected from a Gaussian beam. There is a decrease in ablation depth towards the middle of the spot resulting in a double groove structure. A similar result was obtained by Zhang et al. (2016) on the ablation of grooves of a germanium wafer in water. Furthermore, there are structures which resemble holes at the surface that appear dark in the SEM images. These holes yield a higher contrast for carbon inclusions and may appear due to inclusion of impurities at the surface. The oxygen EDX image does not show any significant changes. In general, the microstructure in water resembles a honeycomb structure. Mostly this structure is obtained by accumulation effects (Mannion et al. (2004)). With increasing spot overlap, the size of these microstructures decreases.

For higher fluences, as expected, the spot size is smaller. The crater possesses a homogenous shape and shows a good quality except of the impurity holes at 0 % OR. At 90 % OR, there might be a slight increase in oxygen contrast in the EDX image. The microstructure again becomes smaller and resembles a melted surface at high OR. This type of surface structure more overly resembles to molten vapor (de Bonis (2013)). Note also that the heat affected zone which is indicated by the change in contrast at the SEM picture is bigger for the ablation at high fluences.

3.3. Properties of ablation in Methanol

Compared to water, the shape of the grooves in methanol is more homogenous at 0.2 J/cm². In contrast to the EDX images of the grooves produced in water, a chemical change of the surface composition is visible in the groove region as a depletion of oxygen in the ablated area. Furthermore, the microstructure possesses a similar structure than in water at 0.2 J/cm² and 0 OR and is also decreasing with increasing spot overlap but keeps the same form.

For 5 J/cm², the grooves are only well visible at 0 % OR meanwhile at higher OR the ablated area resembles more a heat affected zone which has the biggest size at 50 % OR. In contrast to the change of surface composition at 0.2 J/cm², no change of the chemical composition is observed in the EDX contrast image at 5 J/cm². The observed change in surface composition for different fluences is an indication for a fluence dependent chemical reaction during or after the ablation. Furthermore, the microstructure at 0 % OR resembles the structure presented by de Bonis et al. (2013) which looks like the resolidification of a molten explosion. At higher OR, the surface structure is in the sub-micron range and shows a molten structure.

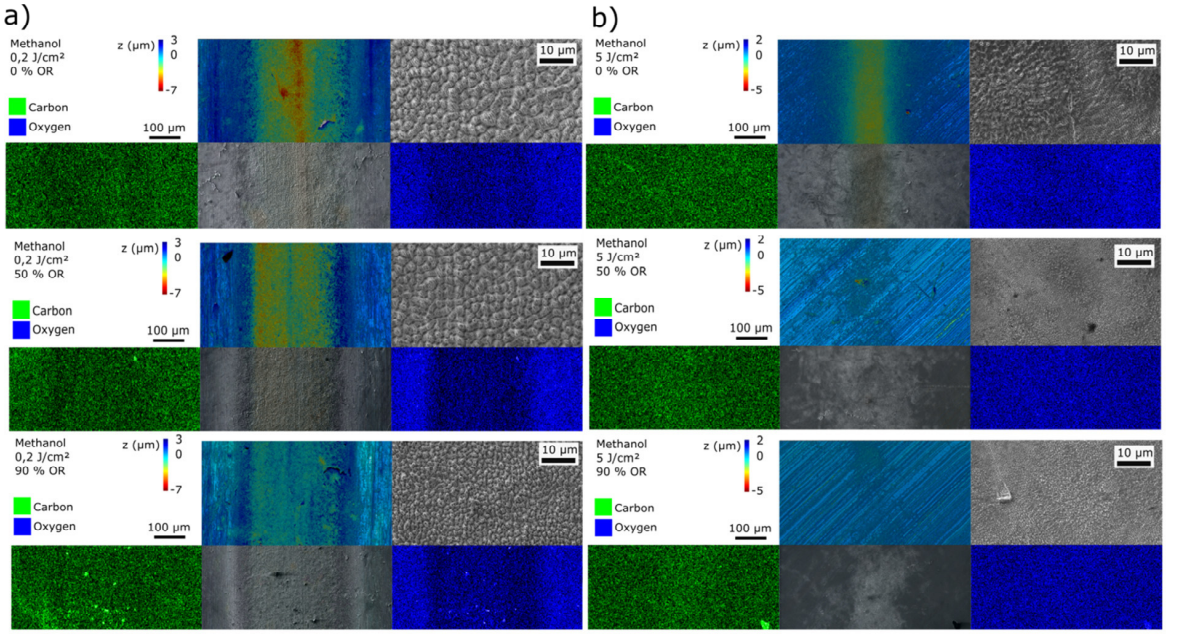

Fig. 3. Properties of the ablated grooves in methanol at a) 0.2 J/cm², b) 5 J/cm².

3.4. Properties of ablation in Ethanol

The general features like the shape and size of the ablated groove and the resulting microstructure in ethanol at 0.2 J/cm² correspond to the observations of the features in methanol (compare Fig. 4 and 5). However, it should be noted that the spot size is changing towards a bigger spot size at a higher OR. Furthermore, a slight change in contrast is also observed for the carbon content from being decrease at 0 % OR to being increased at 90 % OR.

At 5 J/cm², the ablation seems to be homogenous like in methanol and water. However, a strong decrease in ablation rate for increasing OR as for methanol is not observed for ethanol and the ablated area is well visible for 0 and 50 % OR. In addition, the heat affected zone is decreasing with increasing OR although the ablated area is not decreasing. This fact cannot be easily explained as normal shielding should also lead to a decrease in ablated area. In contrast to the ablation at high fluences in methanol, also at higher fluences, a slight depletion of oxygen and a slight increase in carbon concentration is observed.

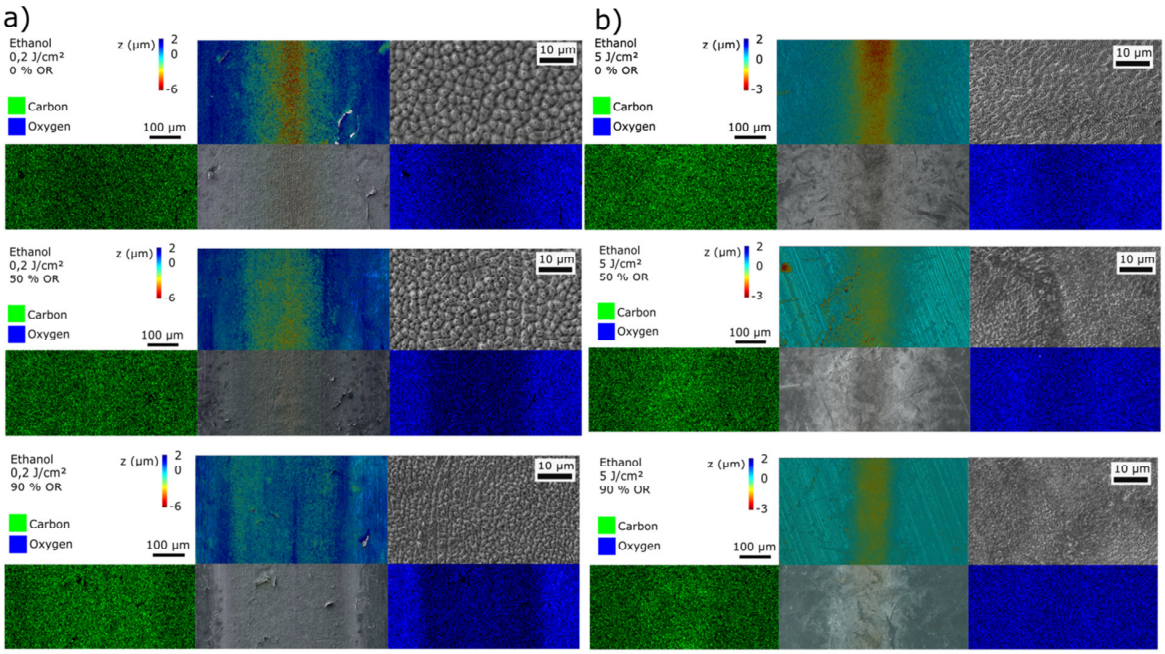

Fig. 4. Properties of the ablated grooves in ethanol at a) 0.2 J/cm², b) 5 J/cm².

3.5. Properties of ablation in Acetone

Fig. 5 shows that the ablation at 0.2 J/cm² in acetone is barely visible. In contrast to the ablation in ethanol, the oxygen depletion increase is less pronounced and decreasing with increasing OR. The carbon concentration at 0.2 J/cm² is slightly increased and exhibits the strongest contrast at 50 % OR. The microstructure is very small and resembles, similar to the grooves ablated at higher fluences in ethanol, a resolidifaction of a molten surface.

For 5 J/cm², the ablation rate is strongly increased and well visible in the SEM picture for an OR of 0 %, but for a further increased OR nearly no ablation is found. Further it seems that the oxygen and carbon concentration are slightly decreased in the ablated area, but this might also be an error of the EDX detector due to the depth of the crater and reabsorption of the x-rays at the groove wall. However, at higher OR, an increase in carbon concentration is detected. The microstructure is very pronounced for 0 % OR, but barely visible for higher OR. For 0 % OR, it shows strong signs of melting. A possibility to explain the high ablation rate might be the low vapor pressure of acetone. By the previous pulse, the local environment is heated up leading to a small sheath of evaporated material reducing the heat transfer from the target to the liquid which leads to a higher ablation rate and more melting.

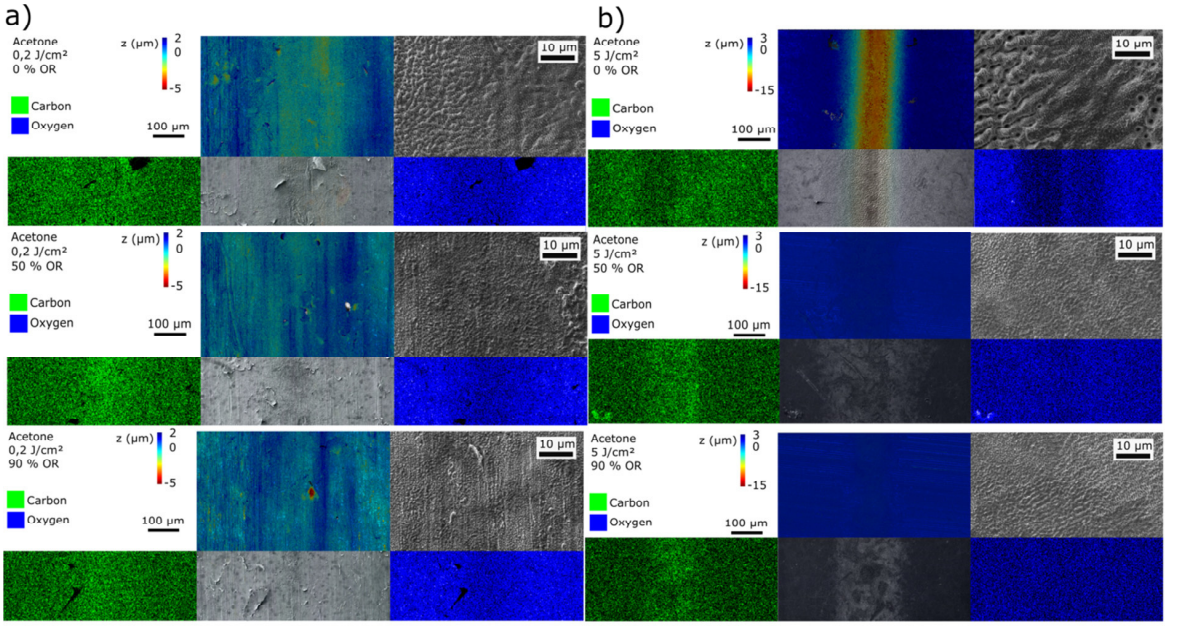

Fig. 5 Properties of the ablated grooves in acetone at a) 0.2 J/cm², b) 5 J/cm².

3.6. Properties of ablation in Toluene

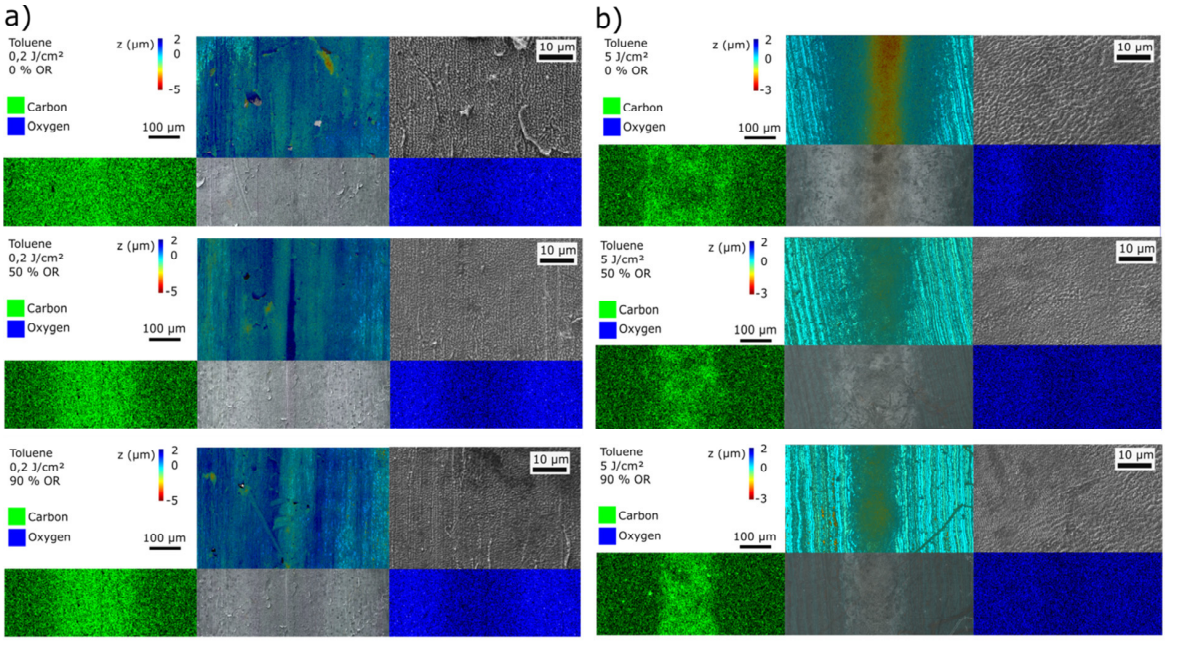

Fig. 6. Properties of the ablated grooves in toluene at a) 0.2 J/cm², b) 5 J/cm².

For 0.2 J/cm², the ablation is barely visible in the white-light interferometer pictures. However, an increasing depletion of oxygen and an increasing concentration of carbon observed in the EDX images indicate that a surface processing took place. Furthermore, there is a regular microstructure on the surface with sub-micron size.

For 5 J/cm², the ablation rate is strongly increased and well visible. At 0 % OR, the carbon content is increasing meanwhile the oxygen content is visibly decreased. At higher OR, the oxygen depletion vanishes. The microstructure is similar to the microstructure at high OR for acetone.

4. Discussion

As shown by this investigation, PLAL is a complex topic, involving several interactions of the target material, liquid and laser beam as can be seen by the different dependencies of the ablation rate with OR as well as microstructure and surface composition of the target. Here, an overview of the influence on the target material is provided for different laser parameters. A summary of the general features is provided in Tab. 1 for 0.2 J/cm² and Tab. 2 for 5 J/cm².

Table 1. Properties of ablation in different liquids at 0.2 J/cm².

Property	Water	Methanol	Ethanol	Acetone	Toluene
Ablation morphology	Not homogeneous	Homogenous	Homogenous	Homogenous	-
Type of microstructure	Micron sized (accumulation effect)	Micron sized	Micron sized	Nano sized (molten vapor)	Nano sized (accumulation)
Surface Chemistry	Impurities	Decrease oxygen	Decrease oxygen	Slight decrease O / slight increase C	Decrease oxygen / increase C

For 0.2 J/cm², it is interesting to note that there is a correlation between ablation rate and microstructure. The size of the microstructure is decreasing with increasing OR. Except the case of water, the mass removal is homogenously distributed over the ablated area. For all used liquids, except of water, a decrease in oxygen contrast was found.

Table 2. Properties of ablation in different liquids at 5 J/cm².

Property	Water	Methanol	Ethanol	Acetone	Toluene
Ablation morphology	Homogeneous	Homogenous	Homogenous	Homogenous	Homogenous
Type of microstructure	Micron sized	Nano sized (molten)	Nano sized	Nano sized	Nano sized
Surface Chemistry	No change visible	Maybe slight oxygen decrease at 0 % OR	Slight decrease oxygen, slight increase carbon	Slight decrease Oxygen	Decrease oxygen, increase carbon

For 5 J/cm², the mass removal is always homogenous. In addition, chemical changes of the surfaces are not as pronounced as for 0.2 J/cm². Consequently, the liquid-substrate interface plays a crucial role.

The here described features are a result of the complex interaction of ablation, liquid and laser beam. This proceeding provides a broad overview of the features which are exhibited by cutting grooves into iron. The two different decreases in ablation rate may be explained by particle shielding and interaction with the cavitation bubble. Further detailed investigations are needed in order to verify the nature of the decrease in ablation rate with different OR as well as the creation of surface structures and chemical surfaces composition.

The change in surface chemistry may be attributed to the creation of highly excited oxygen and carbon species in the ablation plasma which react through different reaction channels either to gas phase molecules, which in the case of oxygen, lead to a depletion of oxygen in the ablated area while carbon, by carbonizing the liquid in the ablated area, is then deposited onto the substrate. For example, nanoparticles generated in toluene are usually surrounded by

an amorphous carbon shell (Intartaglia et al. (2012)). In order to evaluate the nature of the surface chemistry change, surface sensitive techniques such as Raman spectroscopy and XPS need to be applied.

5. Conclusion

Within this proceeding, the influence of different liquids on the ablation of iron at two different fluences of 0.2 J/cm² and 5 J/cm² and different overlapping rates of 0, 50 and 90 % was investigated. For those parameters, the ablation rate, groove morphology and surface composition were investigated in order to provide an overview of the influence of the liquids on the ablation. Thereby, it could be shown that the liquid has a significant influence on all investigated factors. It could be shown that the dependency of the ablation rate on the overlapping rate is affected in two different ways which can be mainly attributed to particle shielding and an interaction with the cavitation bubble. Furthermore, the liquids are strongly altering the surface composition which is an important point for laser processing in liquids. On the one hand, this may lead to unwanted effects like a change of the substrates properties over time or unwanted particle compositions while producing nanoparticles by PLAL. On the other hand, these properties emphasize that liquids and laser parameters provide a useful tool to tailor the ablation process in a desired manner.

Acknowledgements

We gratefully acknowledge the financial funding of the DFG within the Project GU1075/3.

References

Barcikowski, S., Compagnini, G., 2013. Advanced nanoparticle generation and excitation by lasers in liquids. Phys. Chem. Chem. Phys., 15, 3022

Shen, M.Y., Crouch, C.H. Carey, J.E., Mazur, E., 2004. Femtosecond laser-induced formation of submicrometer spikes on silicon in water. Applied Physics Letters 85, 5694

Schaaf, P., 2002. Laser nitriding of metals. Progress in Materials Science 47, 1-161.

Muhammad, N., Lin, L., 2012. Underwater femtosecond laser micromachining of thin nitinol tubes for medical coronary stent manufacture. Applied Physics A, 107, 849.

Zhang, D., Gökce, B., Sommer, S., Streubel, R., Barcikowski, S., 2016. Debris-free rear-side picosecond laser ablation of thin germanium wafers in water with ethanol. Applied Surface Science, 367, 222.

Kruusing, A., 2004. Underwater and water-assisted laser processing. Optical Laser Engineering, 41, pp. 307- 341.

Wagener, P., Schwenke, A., Barcikowski, S., 2012. How Citrate Ligands Affect Nanoparticle Adsorption to Microparticle Supports. Langmuir, 28, 6132.

Nolte, S., Momma, C., Jacobs, H., Tünnermann, A., Chichkov, B. N., Wellegehausen, B., Welling, H., 1997. Ablation of metals by ultrashort laser pulses. Journal of the Optical Society of America B, 14, 2716.

Neuenschwander, B., Jaeggi, B., Schmid, M., Rouffiange, V., Martin, P.E., 2012. Optimization of the volume ablation rate for metals at different laser pulse-durations from ps to fs. SPIE LASE 824307

Wu, C., Zhigilei, L.V., 2014. Microscopic mechanisms of laser spallation and ablation of metal targets from large-scale molecular dynamics simulations. Applied Physics A, 114, 11-32.

Nedialkov, N.N., Imamova, S.E., Atanasov, P.A., 2004. Ablation of metals by ultrashort laser pulses. Journal of Physics D: Applied Physics 37, 638.

Kanitz, A., Hoppius, J., Chakif, M., Gurevich, E.L., Ostendorf, A., 2015. Femtosecond laser ablation of iron in liquid environments. Proceedings of LAMP2015.

Wagener, P., Schwenke, A., Chichkov, B.N., Barcikowski, S., 2010. Pulsed Laser Ablation of Zinc in Tetrahydrofuran: Bypassing the Cavitation Bubble. The Journal of Physical Chemistry C, 114, 7618.

Bonis, A., Lovaglio, T., Galasso, A., Santagata, A., Teghil, R., 2015. Iron and iron oxide nanoparticles obtained by ultra-short laser ablation in liquid. Applied Surface Science, 353, 433.

Bonis, A., Sansone, M., D'Alessio, L., Galasso, A., Santagata, A., Teghil, R., 2013. Dynamics of laser-induced bubble and nanoparticles generation during ultra-short laser ablation of Pd in liquid. Journal of Physics D: Applied Physics, 46, 445301.

Mannion, P.T., Magee, J., Coyne, E., O'Connor, G.M., Glynn, T.J., 2004. The effect of damage accumulation behavior on ablation thresholds and damage morphology in ultrafast laser micro-machining of common metals in air. Applied Surface Science, 233, 275.

Intartaglia, R., Bagga, K., Genovese, A. Athanassiou, A. Cingolani, R., Diaspro, A., Brandi, F., 2012. Influence of the organic solvent on optical and structural properties of ultra-small silicon dots. Physical Chemistry Chemical Physics, 14, 15406.